

Case Study

Reducing CO₂ Bypassing and Optimizing CO₂ Flood Design in Heterogeneous Formation

Marylena Garcia^{1*}, Erwinsyah Putra^{2*§}, Dewi T. Hidayati^{2*} and David S. Schechter^{2*}

Address: ¹Occidental Oil and Gas Corporation, Houston, Texas, USA, ²Petroleum Engineering Department, Texas A&M University, Texas, USA
<http://pumpjack.tamu.edu/Faculty&Staff/faculty/schechter/baervan/homepage.html>

Email: Marylena Garcia marylena_garcia@oxy.com; Erwinsyah Putra - putra@tamu.edu; Dewi T. Hidayati - dewi@tamu.edu; David S. Schechter - schech@spindletop.tamu.edu

*These authors contributed equally to this work

§Corresponding author

Published: 26 September 2005

Received: 15 September 2005

E-Journal of Reservoir Engineering 2005, ISSN: 1715-4677.

Accepted: 20 September 2005

This article is available from: <http://www.petroleumjournals.com/>

© 2005 Garcia et al; licensee Petroleum Journals Online.

This is an Open Access article distributed under the terms of the Creative Commons Attribution License (<http://creativecommons.org/licenses/by-nc-nd/2.0/>), which permits unrestricted use for non-commercial purposes, distribution, and reproduction in any medium, provided the original work is properly cited.

Abstract

This research utilized a modeling approach to reduce oil bypassed in CO₂ flood pattern. A fully compositional simulation model with detailed geological characterization was developed to optimize the flood pattern. The simulation model is a quarter of an inverted nine-spot and covers 20 acres area. The Peng-Robinson equation of state (EOS) was used to describe the phase behavior during CO₂ flooding. Simulation layers represent actual flow units and resemble large variation of reservoir properties. A-27 year production and injection history was matched to validate the model. Then, several sensitivities run including CO₂ injection rate, slug size, WAG ratio, pattern reconfiguration and conformance control were conducted to improve CO₂ sweep efficiency and increase oil recovery.

We found that the optimum CO₂ injection rate is approximately 300 RB/D (762 MSCF/D). The optimum water-alternating-gas (WAG) ratio is 1:1. This ratio allows an incremental oil recovery up to 18% with an ultimate CO₂ slug of 100% hydrocarbon pore volume (HCPV). If a polymer is placed in high permeability streak during the course of 1:1 WAG ratio, an additional recovery could increase up to 34%. The simulation results also reveal that a pattern reconfiguration change from inverted nine spot to staggered line drive could significantly increase oil recovery.

Introduction

CO₂ injection has been known as an effective solvent to improve oil recovery for a number of reasons. In general, CO₂ is very soluble in crude oils at reservoir pressures; therefore, it swells the oil and reduces oil viscosity. The effect of CO₂ is more pronounced when the pressure achieves minimum miscibility pressure (Martin and Taber, 1992). Miscible gas injection has been implemented successfully in a number of fields around the world (Rogers and Griggs, 2000). Miscible gas injection has excellent microscopic sweep efficiency but poor macroscopic sweep efficiency due to viscous fingering and gravity

override. To increase sweep efficiency during gas injection, Water Alternating Gas (WAG) process has been implemented. In practice the WAG process consists of the injection of water and gas as alternate slugs by cycles or simultaneously (SWAG), with the objective of improving the sweep efficiency of waterflooding and miscible or immiscible gas floods projects.

The mobility ratio between injected gas and the displaced oil bank by CO₂ and other miscible gas displacement processes is typically very unfavorable because of the relative low viscosity of

the injected phase. A very unfavorable mobility ratio results in viscous fingering and poor sweep efficiency. The WAG process is an injection technique developed to overcome this problem by injecting specified volumes, or slugs, of water and gas alternatively. As results of this process, the mobility of the injected gas alternated with water is less than that of the injected gas alone, and thus the mobility ratio of the process is improved.

In WAG injection, water/gas injection ratios have ranged from 0.5 to 4.0 volume of water per volume of gas at reservoir conditions. The sizes of the alternate slugs range from 0.1% to 2% of the pore volume (PV) (Huang and Holm, 1988). Total or cumulative slug sizes of CO₂ in reported field projects typically have been 15% to 30% of the hydrocarbon pore volume (HCPV), although smaller and larger slugs have been reported (Green and Willhite, 1998). The main factors affecting the WAG injection process are the reservoir heterogeneity, rock wettability, fluid properties, miscibility conditions, gas trapped, injection technique and WAG parameters such as slug size, WAG ratio and injection rate (Sanchez, 1999).

Reservoir heterogeneity and stratification have a strong influence on the water/gas displacement process (Sanchez, 1999). The degree of vertical reservoir heterogeneity can affect the CO₂ performance. Reservoirs with higher vertical permeability are influenced by cross-flow perpendicular to the bulk flow direction (Kulkarni and Rao, 2004). Cross-flow may increase the vertical sweep, but generally the oil recovery is low due to the gravity segregation and decreased flood velocity in the reservoir. Reservoir heterogeneity controls the injection and sweep patterns in the flood. Reservoir simulation studies for various kv/kh (vertical to horizontal permeability) ratios suggest that higher ratios adversely affect oil recovery in WAG process (Jackson *et al.*, 1985). In highly stratified reservoirs, the higher permeability layer(s) always respond first, resulting in an early breakthrough and poor sweep efficiency. For these heterogeneous reservoirs, a WAG process would reduce the mobility in the high permeability layer, resulting in a larger amount of the CO₂ contacting the crude oil in that particular layer. If heterogeneity has adversely affected waterflood sweep, a CO₂ flood using the same pattern is very likely to be unsuccessful.

Well injection patterns and well spacing also have a great impact on the sweep efficiency in a CO₂ flood. The pattern injections most popular in the field are the 5-spot pattern and the inverted 9-spot patterns. The 5-spot pattern gained high popularity in field operations during CO₂ floods because its well spacing makes it attain better flood front control and

help to maintain higher average reservoir pressure (Jarrel *et al.*, 2002). The inverted 9-spot pattern was also very common in the early years of many CO₂ floods in west Texas (Thai *et al.*, 2000; Harpole and Hallenbeck, 1996). Regardless of the type of pattern used for a CO₂ flood, it is very important and critical that there are no major volumetric sweep problems under the operations. Problems with low reservoir pressure and poor sweep efficiency during a waterflooding will definitely get worse during a CO₂ flooding (Jarrel *et al.*, 2002).

When a WAG has failed to control sweep, other techniques such as surfactant foams, gel polymers and conventional plugging methods can be used to improve the sweep efficiency of the injection process (Jarrel *et al.*, 2002; Chakravarthy *et al.*, 2004). The objective of gel treatments and similar blocking-agent treatments is to reduce channeling through fractures or high-permeability zones without significantly damaging hydrocarbon productivity. The idea is to achieve a permeability reduction in high permeability layers, while minimizing gel penetration and permeability reduction in less-permeable, hydrocarbon-productive zones. This objective can be met by mechanically isolating zones during the gel-placement process, so that gel injection occurs only in the high-permeability zones (Holm, 1987; Chakravarthy *et al.*, 2004). If analogous flood suggests that premature water/CO₂ breakthrough will be a problem, or representative core data indicate that the reservoir will not flood uniformly, polymers or blocking agent treatments should be carried out to avoid sweep efficiency problems. Expected results are more oil produced faster and at lower gas-oil ratios.

Denver Unit Overview. The Wasson Field is situated in Gaines and Yoakum counties on the southeastern margin of the northwest shelf of the North Basin Platform of the Permian Basin in West Texas (Mathis, 1986) (**Fig. 1**). Wasson Field was discovered in 1936. The Denver Unit is the largest unit in Wasson Field and is the world's largest carbon dioxide enhanced oil recovery (EOR) project. The 27,848 acre Denver Unit is located in the southern edge of North Basin Platform of the Permian Basin in West Texas (**Fig. 1**).

The unit produces from the San Andres Formation, a middle Permian-aged dolomite located at subsurface depths ranging approximately from 4,800 to 5,200 ft. The Denver Unit initially contained more than 2 billion barrels of oil in the oil column (OC), which is the interval of the San Andres hydrocarbon accumulation above the producing oil/water contact (OWC). The field's

producing oil water contact (POWC), above which oil is produced water free during primary recovery, varies from -1,250 ft to -2,050 ft below sea level. Above the POWC, petrophysical data generally show that oil occupies the pore space unsaturated by the reservoir connate water. San Andres formation contains more than 650 million bbl of oil in a transition zone (TZ), which is the interval between the OWC and the true water level, commonly known as the base of zone (BOZO). The transition zone saturation, 35-65% was not effectively recovered by primary and waterflood primary methods. At Denver Unit, the transition oil has been proven to be an economical CO₂ enhanced oil recovery target (Hsu *et al.*, 1995; Ghauri, 1979; Thai *et al.*, 2000).

The Wasson San Andres field contains a primary gas cap. The subsea depth of the initial gas/oil contact (GOC) was estimated to be -1,325 ft when the field was unitized in 1964. Because San Andres Formation in the Denver Unit is stratigraphically highest among all units operating the Wasson Field, more than 90% of the gas cap resides within the western portion on the Denver Unit (Hsu *et al.*, 1995).

Primary depletion drive production began in 1936 with single well production rates greater than of 1500 STBD. In 1964, the Denver Unit was formed and a waterflooding was initiated. Peak secondary oil production of 37,100 BOPD occurred in 1975 (Ghauri, 1979). CO₂ injection began in 1983, when nine inverted nine-spot patterns were placed on CO₂ injection (Fleming *et al.*, 1992). CO₂ was initially injected into the eastern half the unit. Flood patterns were regularized with infill drilling to become inverted nine spot patterns. From 1989 to 1991, CO₂ injection was expanded areally to include

most of the western half of the field. In 1994, the area of the field with the highest transition zone oil in place also began CO₂ injection (Thai *et al.*, 2000). Today, over 400 million cubic feet per day of CO₂ are injected into 185 injector wells within the 21,000-acre project area, while 38,000 bbl of oil per day are produced (**Fig. 2**).

Problem Description. The paper addresses the effects of heterogeneity on the overall sweep efficiency. Due to the heterogeneity of the formation, the response to the CO₂ injection varies across the field affecting the overall sweep efficiency. This has caused poor sweep efficiency and also the bypassing of considerable amount of oil by the CO₂.

A reservoir simulation model will be used to optimize CO₂ injection rates, evaluate different CO₂ injection patterns, to determine the optimum WAG ratio, evaluate the use of a viscous agent in WAG application, and to improve conformance control by applying polymer injection via compositional simulations in section 48 of Wasson San Andres formation.

Objectives. The main goal of this work is to provide the best methodology to improve the sweep efficiency of miscible CO₂ floods and enhance the conformance control in section 48 in the San Andres formation, Wasson Field. The main objectives of this work will also include: (1) determining the optimum CO₂ injection rates and WAG ratios; (2) investigating the effect of conformance control on the ultimate oil recovery; (3) studying the effect of pattern changes on the sweep efficiency

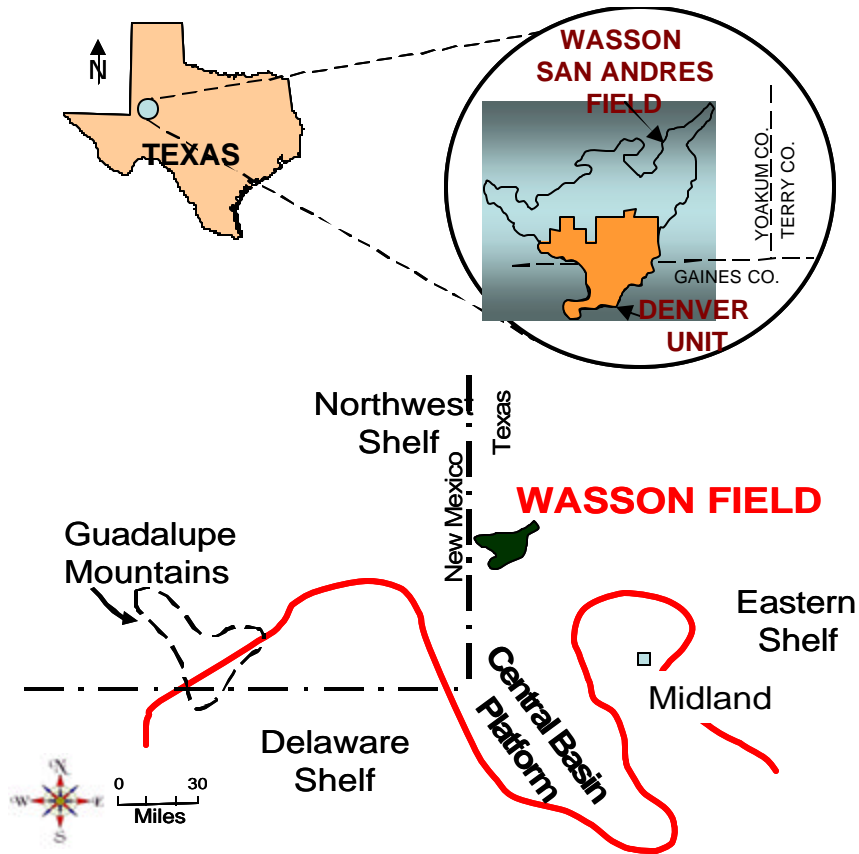


Fig. 1—Location of Wasson field in the Permian Basin (Mathis and Sears,1984)

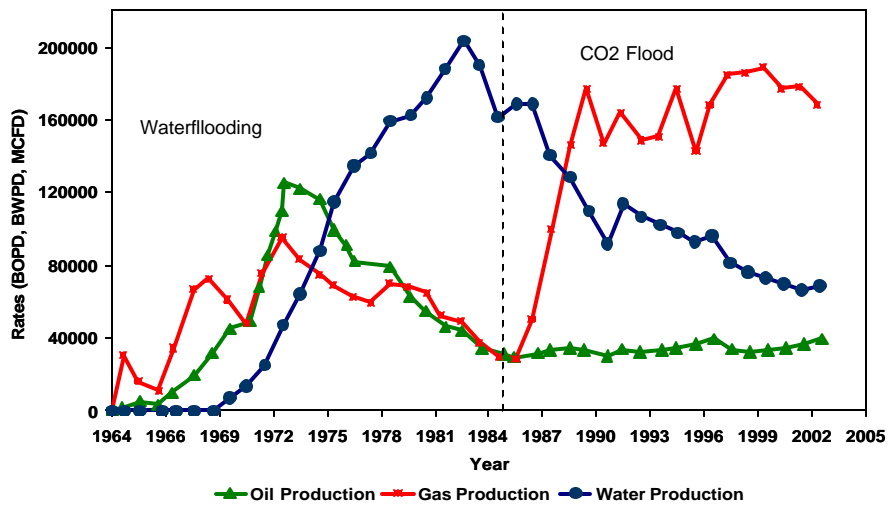


Fig. 2—Denver Unit - Production Performance (Thai *et al.*, 2000)

Simulation Model Construction

The reservoir model for the simulation study is a quarter of an 80-acre inverted nine spot pattern.

The model covers 20 acres and contains 3 production wells and one injection well (**Fig. 3**). Production and injection wells are vertical and completed in all the layers of the simulation model.

The reservoir properties can be seen in **Table 1**. The grid sensitivities were conducted to obtain minimum requirement of the grid block numbers. We obtained that the 20 x 20 grid number provides satisfactory results when compared to finer gridded models. An existent geologic description (Mathis, 1986) was used to define the layers of the simulation model (**Fig. 4**). Simulation layers were constructed to represent the actual reservoir zonation and resemble actual flow units. Each layer properties such as thickness, porosity and permeability were taken from an existing petrophysical evaluation of the area (**Figs. 5 and 6**). There are no areal variations of thickness, porosity and permeability across each single simulation layer.

Table 1—Basic reservoir properties

Formation	San Andres
Top of Pay (ft)	5000
Pay Thickness (ft)	292.5
OOIP (MMSTB)	>2.0
Average Porosity (%)	0.115
Average Permeability (md)	5.67
Initial Reservoir Pressure (psi)	1805
Bubble Point Pressure (psi)	1805
Reservoir Temperature (°F)	105
Minimum Miscibility Pressure (psi)	1300

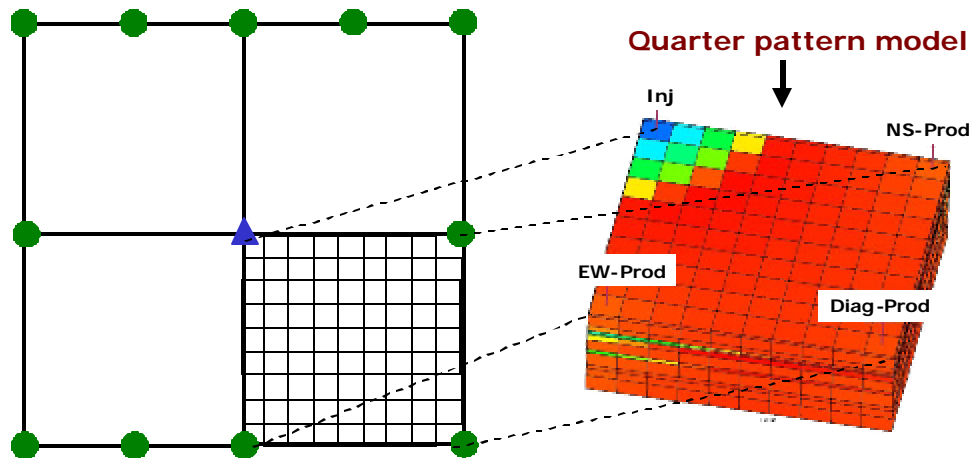


Fig. 3—Well pattern geometry

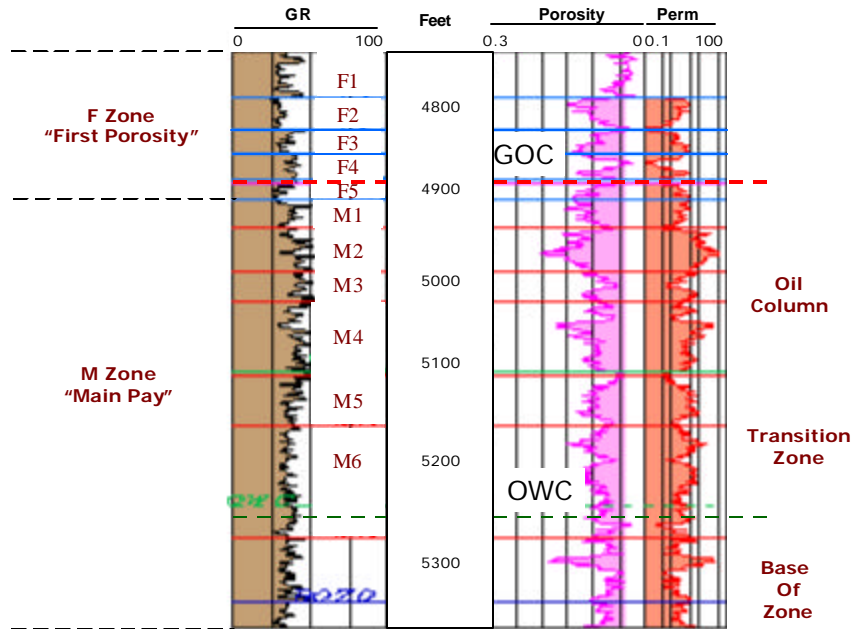


Fig. 4—Type log Denver unit (Mathis, 1986)

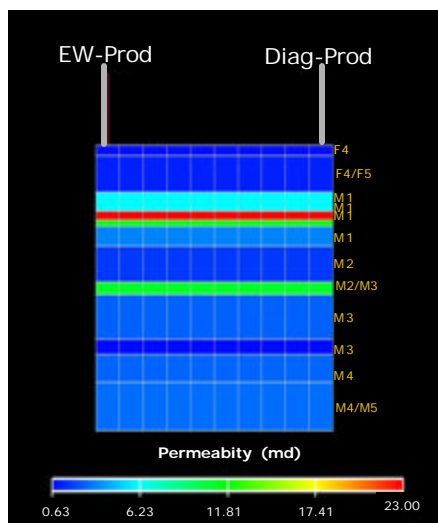


Fig. 5—Variation of permeability values at each layer

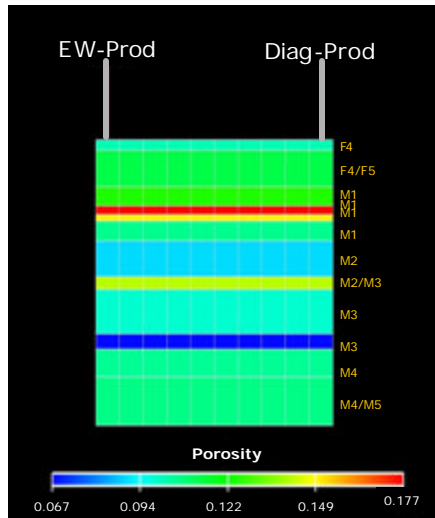


Fig. 6—Variation of porosity values at each Layer

Table 2—Reservoir Fluid Composition in Mole Fractions

CO ₂	N ₂	C ₁	C ₂	C ₃	i-C ₄	n-C ₄	i-C ₅	n-C ₅	C ₆	C ₇₊
0.0297	0.0040	0.0861	0.0739	0.0764	0.0095	0.0627	0.0159	0.0384	0.0406	0.5628

Temperature, °F: 105
 C7+ Molecular weight: 229
 C7+ Density @ 60 °F, gr/cm3: 0.88

Fluid Properties. The reservoir oil is a saturated black oil with a stock tank gravity of 33° API and an initial GOR of 660 SCF/STB. Initial reservoir pressure and bubble point pressure is 1,805 psi at a reference depth of 5,000 ft and 105°F (see **Table 1**). The CO₂ minimum miscibility pressure was determined experimentally to be 1,300 psi. **Table 2** shows the fluid composition.

PVT Equation of State Characterization. An essential part of a compositional reservoir simulation of a miscible EOR method is the prediction of the complex phase equilibria during EOR processes (Merrill *et al.*, 1994). An equation-of-state (EOS) was tuned to reproduce the observed fluid behavior and to predict the CO₂ /oil phase behavior in the compositional simulation (Khan *et al.*, 1992).

PVT laboratory sample data of the San Andres formation were used in the tuning of the EOS. PVT laboratory data consists of differential liberation (DL) experiments, constant-composition-expansion (CCE), and swelling test. These data were used to tune an EOS that is capable of characterizing the CO₂/reservoir-oil system above the minimum

miscibility pressure (MMP). Each laboratory experiment was simulated with the cubic Peng Robinson EOS without performing any regression and compared to the laboratory observations (PVT) (Peng and Robinson, 1976). The preliminary results after the simulation were fairly good, demonstrating that the behavior of the fluid was being reproduced with a basic (not yet tuned) EOS; however, some experiments were not fully matched. This was a clear indication that the parameters of the EOS needed some adjusting in order to reproduce the behavior of the reservoir fluid.

Next step was to tune or characterize the EOS so that it is able to reproduce the PVT experiments. This was a multi-step process that was started by the splitting the heavy component as proposed by Whitson (1983) (**Table 3**). Whitson's method uses a three-parameter gamma probability function to characterize the molar distribution (mole fraction / molecular weight relation) and physical properties of petroleum fractions such as heptanes-plus (C₇₊). This method is used to enhance the EOS predictions.

Table 3—EOS Characterization

<u>Original Composition</u>	<u>"After Split "</u> <u>Composition</u>	<u>Tuning</u> <u>of EOS</u>	<u>"After Grouping"</u> <u>Composition</u>
CO ₂	CO ₂	<div style="border: 1px solid black; border-radius: 15px; padding: 10px; text-align: center;"> Regressions on the C₇₊ pseudo components Regressed Variables: { Critical Temp. Critical Press. Acentric Factors BIC's </div>	6 components CO ₂ (N ₂ - C ₁) (C ₂ - C ₃) (iC ₄ - nC ₄) (C ₅ - C ₆) C ₇₊
N ₂	N ₂		
C ₁	C ₁		
C ₂	C ₂		
C ₃	C ₃		
iC ₄	iC ₄		
nC ₄	nC ₄		
iC ₅	iC ₅		
nC ₅	nC ₅		
C ₆	C ₆		
C ₇₊	C ₇₊₍₁₎ C ₇₊₍₁₎ C ₇₊₍₁₎		

The heavy component (C₇₊) was split into three pseudo components based on its relative mole fraction as suggested by Khan *et al.* (1992). The pseudo components were identified as C₇₊₍₁₎, C₇₊₍₂₎ and C₇₊₍₃₎. By splitting the heavy component (C₇₊), the total number of components of the reservoir fluid was then incremented from 11 to 13 components. This 13-component mixture was used to tune the EOS by regressions to match the observations. Since a single heptanes-plus (C₇₊) fraction lumps thousands of compounds with a carbon number higher than seven, the properties of the heavy component C₇₊ are usually not known precisely, and thus represent the main source of error in the EOS and reducing its predictive accuracy. For this reason, regressions were performed against the pseudo components to improve the EOS predictions. Several regressions were carried out during the process of tuning the EOS. The first regression was performed on all the experiments against the critical pressure of the pseudo components, C₇₊₍₁₋₃₎. The results provided very good predictions with little error when compared against the observations and EOS predicted the observations (PVT data). In general, the regression parameters were basically the C₇₊₍₁₋₃₎ pseudo components critical pressure (P_c), critical temperature (T_c), acentric factor (ω) and binary interaction coefficients (δ). The shift parameters of the C₇₊₍₁₋₃₎ pseudo components were also regressed together, so that changes within the C₇₊ fraction were consistent.

For the simulation of CO₂ miscible EOR processes, the EOS must be capable of predicting phase equilibria over a wide range of CO₂ compositions.

For this reason, CO₂/hydrocarbon binary interaction parameters (BIC) were numerically regressed to achieve the match of the swelling test experimental data.

After a satisfactory match of all the experimental data, the next step was to group the 13-component EOS into a reduced pseudo component EOS acceptable for a compositional simulation. By doing this reduction, the computational time constraint and the numerical complexity of the simulation were expected to be minimized.

The methodology for a stepwise regression presented by Fevang *et al.* (1983) was used for the lumping process from 13 to 10 components. The lumping process consisted of forming new pseudo components from existing components. Then, regressions were performed to fine-tune the newly-formed pseudo component EOS properties. This process was repeated a number of times to select the best grouping at each stage in the pseudoization process. Since various combinations of grouped components are possible, the criterion for grouping was selecting components with similar properties and molecular weight and to have as few components as necessary to match the PVT experiments. A series of grouping exercises were performed. First, a 10-component EOS model was obtained after grouping C₁+N₂, i-C₄+n-C₄, and i-C₅+n-C₅, leaving the remaining components ungrouped.

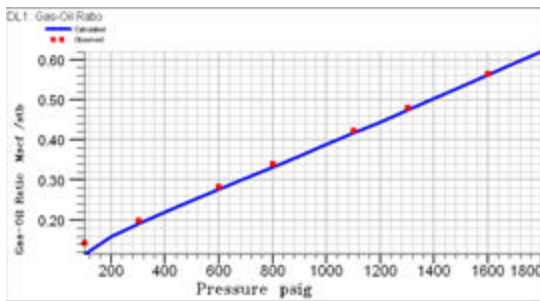
The regression parameters to tune the EOS were the critical properties of the newly-formed pseudo-components. After performing these

regressions, the PVT properties of the 10-component EOS model matched the 13-component EOS model almost exactly.

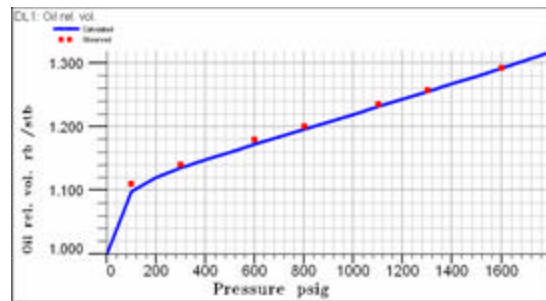
From the 10-component EOS model, another grouping was conducted. The C_{7+} pseudo components, $C_{7+}(1-3)$, were grouped into a single fraction (C_{7+}). Additionally, $C_2 + C_3$ and $i-C_4 + n-C_4 + i-C_5 + n-C_5 + C_6$ were also lumped together. With this grouping a 6-component EOS model was obtained. The 6-component EOS model contained the following components: (CO_2); (N_2, C_1); (C_2, C_3); (C_4); (C_5-C_6), and (C_{7+}). Regression was performed again, and the 6-component EOS model predicted PVT properties very similar to the 10-component

EOS model. This EOS was accepted for use in simulation.

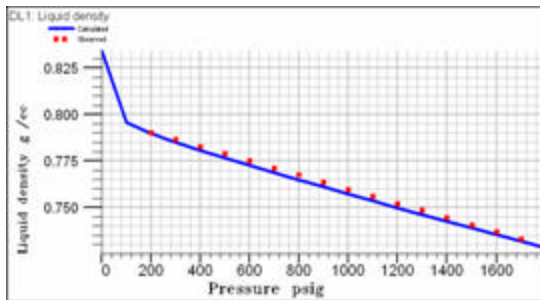
As a final step, regression was performed against both gas and oil viscosity to ensure correct estimation of reservoir fluid viscosity. Regressions against the critical-volume (Z_c) variable were carried out to predict realistic values of viscosity. **Fig. 7** shows the results of the tuning of the EOS. After a satisfactory match of all the experimental data, a grouping procedure was performed with some of the components of the EOS to get an EOS acceptable for a compositional simulation. By doing this reduction, the computational time constraint and the numerical complexity of the simulation were expected to be minimized.



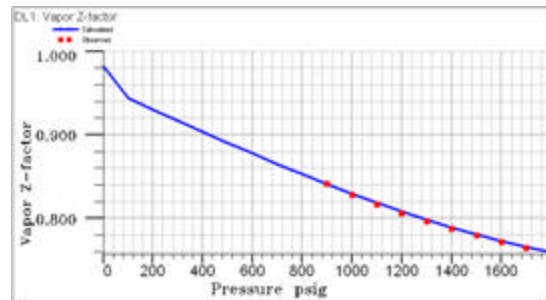
(a) GOR



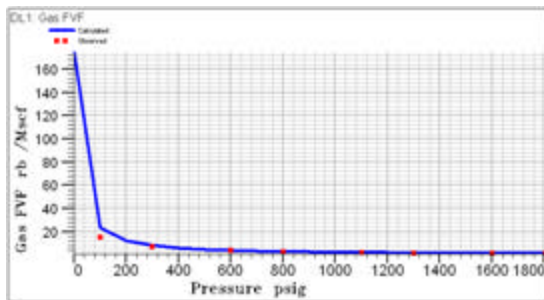
(b) FVF



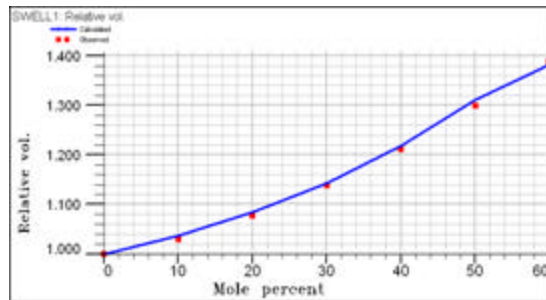
(c) Oil density (ρ_o)



(d) Gas deviation factor (Z)



(e) Gas FVF



(f) CO_2 swelling factor

Fig. 7—PVT EOS results between observed data and simulated results

Relative Permeability. Relative permeability is an important petrophysical parameter as well as a critical input parameter in simulation of miscible floods. However, relative permeability is a lumping parameter and includes the effects of wetting characteristics, heterogeneity of reservoir fluids and rock and fluid saturations (Rogers and Grigg, 2000). Laboratory floods attempting to emulate CO₂ flood (Christman and Gorell, 1988) experienced appreciable water relative permeability reductions after CO₂ injection. In addition, the data shows significant hysteresis effects in the water relative permeability between the drainage and imbibition curves (Rogers and Grigg, 2000).

The two phase oil-water at $S_g = 0$ and gas-oil relative permeability curves used for the waterflood simulation are shown in **Figs. 8 and 9**. The relative permeability data are based on laboratory analyses.

During a WAG injection, each cycle of water injection is of an imbibition type, whereas as soon as gas injection begins the process will switch to the drainage flow. Therefore, the hysteresis effects have to be considered. Hysteretic effects on the relative permeability curves were included in the simulation

model to consider the impact of saturation cycles as water and gas slugs move through the reservoir. **Fig. 8** shows the imbibition and secondary drainage curves relative permeability curves used in the simulation model for the WAG process. The major characteristic of the hysteresis curve is the increase in the connate water saturation from 15% on imbibition to 25% on secondary drainage. This increase occurs because the water is trapped by the wetting oleic phase during the secondary drainage. This trapped water reduces the water relative permeability on secondary drainage and also reduces the oil end-point relative permeability.

History Matching

The pattern was history matched for both waterflood and CO₂ flood. The oil production and injection rates were specified in each well and the model reproduced the reservoir pressure, and the gas and water production. The quality of the history match was judged from how well the simulated water and gas production compared to the historical data.

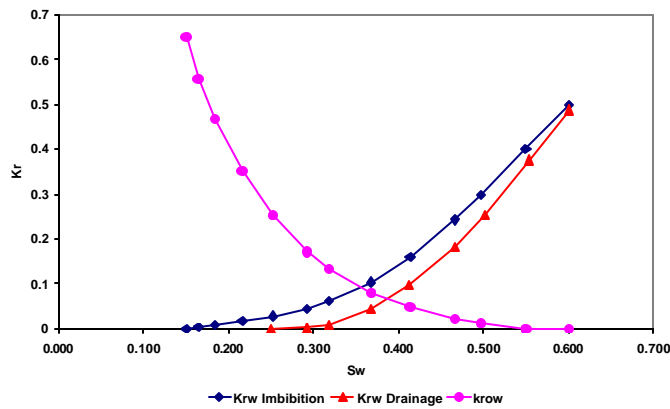


Fig. 8—Imbibition and secondary drainage water relative permeability (hysteresis)

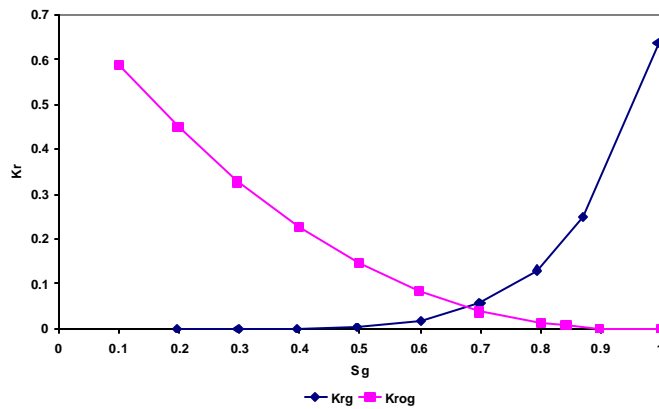


Fig. 9—Gas and oil relative permeability curves as a function of gas saturation

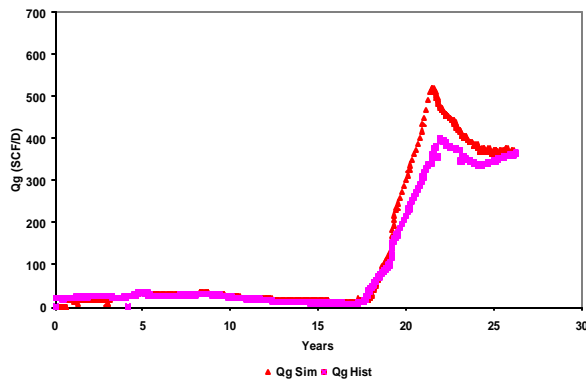
For the history match, the relative permeability curves were slightly adjusted to obtain a better producing water-to-oil ratio (WOR).

Additionally, well connection factors to the simulation grid were modified based on the fact that most of the wells have been fractured and the wells permeability-thickness product, kh , and the skin factor, S , were unknown. Since the connection factor is calculated based on the cell properties, cell geometry and completion information, modification of the connection factor was accomplished by enlarging the completion interval of the production wells to account for the effect of hydraulic stimulation.

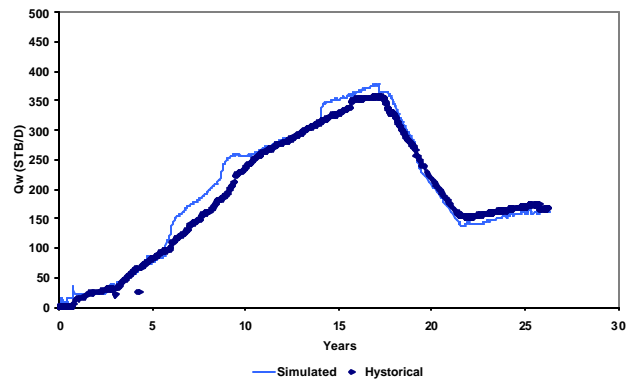
During the WAG process, equal volumes of water and gas (at reservoir conditions) were injected

during each slug resulting in a WAG ratio (volume of water to that of gas in a slug) of approximately 1. This WAG ratio was kept constant for the CO_2 flood historymatch.

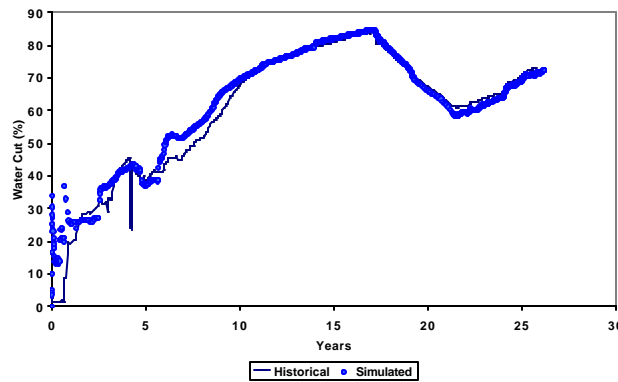
During the waterflood period, water cut match deviates at early times. However, the overall water production matches very well. A reasonable match of gas production was also obtained. **Fig. 10** shows the comparison between historical data and simulation results of gas and water production during the history match period. Oil and water production matches from individual wells were also very good. These indicate that the simulation model was properly calibrated and can be used to predict reservoir performance.



(a) Gas production history match



(b) Water production history match



(c) Water cut history match

Fig. 10—History match between observed data and simulation results

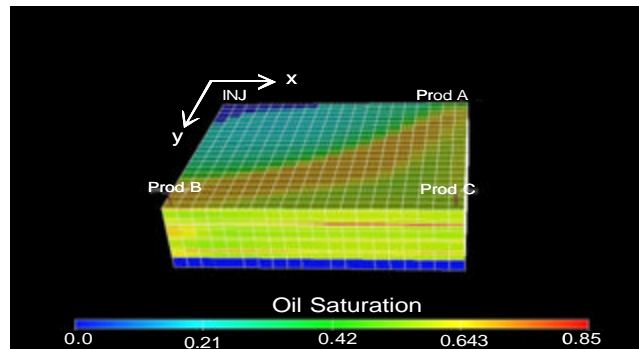


Fig. 11—Areal view of the oil saturation distribution

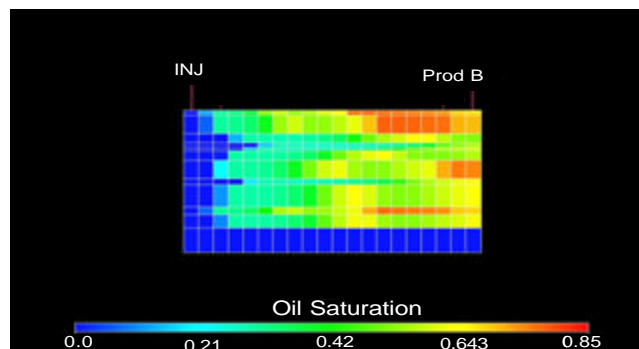


Fig. 12—E-W cross section view of the oil saturation distribution

At the end of the history match period, the average remaining oil saturation was 45%. **Fig. 11** shows the distribution of oil saturation at the end period. It shows that there are many unswept area between an injector and producers. The channeling of the injected fluids within the reservoir is clearly seen in the cross sections (**Fig. 12**). The channeling causes a non-uniform movement of the front and thus creates poor sweep efficiency. High-permeability layers breakthrough earlier than the low-permeability layers, leaving some untapped reserves behind.

The pattern experienced a severe breakthrough which reduced the overall sweep efficiency of the pattern. Additionally, little oil displacement was observed in the upper layers of the simulation model. The sweep efficiency of the patterns was merely impacted by the contrast in permeability between the upper and lower layers of the formation. As a result, most of the injected fluids moved into the lower layers even though the upper layers have commercial permeability.

Results of the simulation do not only highlight reservoir areas with high oil saturation to the future CO₂ flooding but also reveal that mobility ratio needs to be improved and the breakthrough has to be controlled in order to improve the sweep efficiency and increase the incremental oil recovery of the pattern.

Results and Discussion

CO₂ Injection Rate Optimization. To investigate the effect of the injection rate on the WAG process four sensitivities were performed at a WAG ratio of 1:1 using constant rates of 100, 200, 300 and 500 RB/D (233.5, 467, 762 and 1167 MSCF/D respectively) of CO₂. 3% HCPV half cycle of CO₂ and 3% HCPV half cycle of water were injected until a fixed total CO₂ slug of 30% HCPV was reached. It can be seen that the recovery from WAG changes as a function of the injection rate.

Fig. 13 indicates that the optimum injection rate for a 1:1 WAG ratio is between 200 and 300 RB/D.

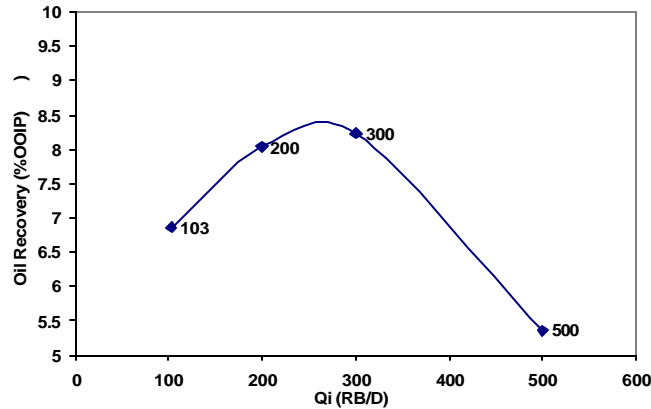


Fig. 13—Comparison of oil recovery obtained at different injection rates

Optimum Water-Alternating-Gas (WAG) Ratio. Two of the most important design issues for WAG process optimization are the WAG ratio and the amount of gas injection or slug size. Various compositional simulations were conducted to determine the optimum WAG ratio and the optimum slug size. A series of WAG ratio sensitivities were compared. Water-alternating with CO₂ injections at four different WAG ratios (1:1, 1:2, 2:1, and 4:1) were performed. The runs evaluated CO₂ slug sizes up to 100% HCPV. The gas and water injection were carried out in cycles injecting both fluids in the same well.

Results indicate that injecting a 100% hydrocarbon pore volume (HCPV) slug of CO₂ with a 1:1 WAG ratio would yield the maximum incremental oil recovery. The design included injection of alternating volumes (3.0% HCPV) of CO₂ and water

into each pattern until the target 100% slug size is reached.

Fig. 14 shows the CO₂ flood performance for the different WAG ratios as a function of total CO₂ injection. It also shows a continuous CO₂ flood and waterflooding recovery profiles. The recovery profiles obtained indicates that the best incremental oil recovery is obtained with a WAG ratio of 1:1. The incremental oil recovery obtained with the continuous flood was low due to early breakthrough of CO₂ injection through high permeability layers of the pattern.

Fig. 15 shows the residual oil saturation in the reservoir for all the cases after 100% HCPV have been injected. As expected, the 1:1 WAG ratio exhibits the lowest remaining oil saturation.

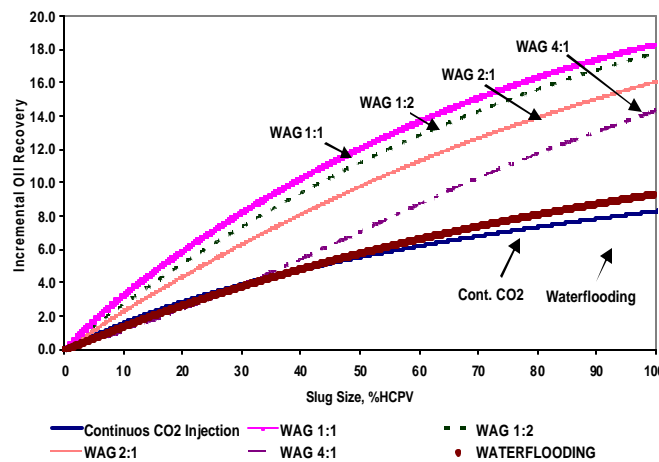


Fig. 14—Comparison of incremental oil recovery between different WAG ratios

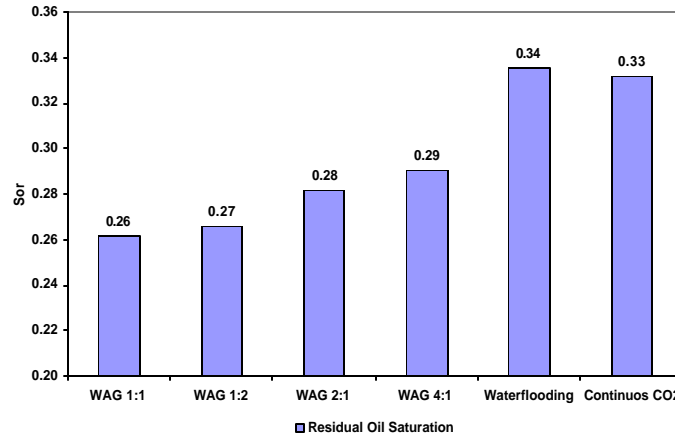


Fig. 15—Comparison of the residual oil saturation for different WAG ratios after 100% HCPV injection

Conformance Control. Channeling of the injected CO₂ during a WAG process has been a major area of concern in the oil industry (Rogers and Grigg, 2000). During the course of CO₂ injection multiple profile control treatments have been conducted to improve the sweep efficiency.

In order to reduce the CO₂ mobility and delay the breakthrough of the CO₂, simulations of a blocking agent and a viscous water treatment were performed with a WAG ratio of 1:1. This simulation allowed for the investigation of the effect of these treatments on the sweep efficiency and conformance control.

A blocking agent, such as gel, must be selectively injected so that it flows to the most permeable zones. After a certain amount of time, the gel stiffens and blocks fluid through those zones. Polymer injection reduces CO₂ cycling through a high permeability layer between the injection well and offset producing wells. To simulate the effect of placing the blocking agent in the “thief” zone, a high permeability layer was identified in the simulation model and the gridblock next to the injector well

was plugged by assigning it a zero permeability value (Fig. 16).

For the viscous water treatment, the injected water viscosity was increased from 1 to 20 cps. For this run, care was taken not to increase the injection pressure above the formation parting pressure in order to avoid an induced fracture. The incremental recovery obtained from the gelled polymer injection and the viscous water treatments are compared to the recovery obtained from a WAG 1:1 ratio injection process without any treatments. The oil production rate of the pattern exhibits a significant response to the treatments performed on the injection well (Fig. 17).

Even though results indicates that the application of these treatments can significantly increase the oil production, the success of this technique in the field will depend on the correct placement of the polymer without damaging other adjacent layers. Additionally, it depends on the periodic repetition of the treatment to positively affect areal sweep efficiency.

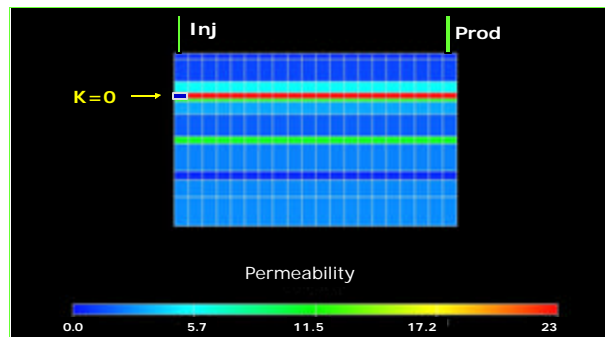


Fig. 16—East–West cross section view of the model showing the permeability blocked by the polymer

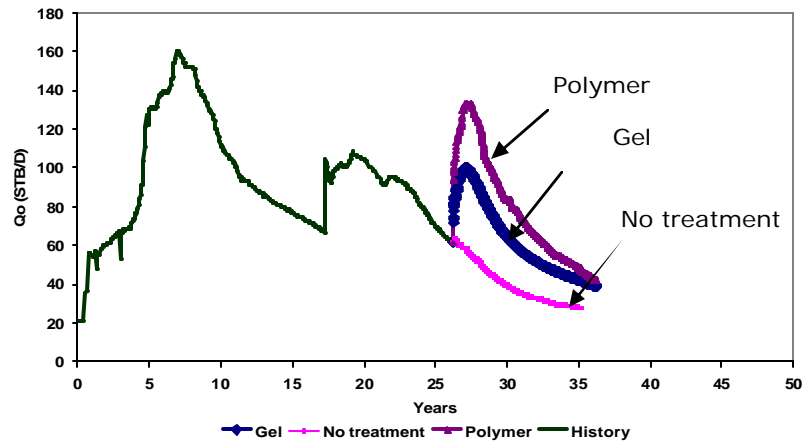


Fig. 17—Comparison of oil rate obtained from different conformance control treatments

Optimum Well Pattern. This section analyzes the effect of pattern reconfiguration on the CO₂ displacement. Pattern conversion is a viable option to achieve an incremental recovery in a mature field with high remaining oil saturations.

A pattern reconfiguration can improve the performance by improving the geometry, decreasing the spacing of the patterns, reducing the producer/injector ratio, and hence improving areal and vertical efficiency. This sensitivity includes infill drilling and well conversion from producer to injector to achieve a better CO₂ displacement throughout the reservoir and ultimately obtain a substantial increase in production from the existing CO₂ flood.

Different well pattern configurations were simulated and analyzed. The inverted nine-spot pattern was converted into different patterns such as a staggered

line drive pattern, line drive pattern and a nine-spot pattern. **Fig. 18** shows the geometric patterns considered in this work. The gridded zone represents the simulated area of the full pattern. The forecasting using these patterns was started at the end of the history match and run for about 25 years.

Figs. 19 and **20** compare the production performance obtained from each pattern investigated. The sharp rise in the production rate is very evident after redefining the well pattern geometry to staggered line drive and line drive patterns. Simulation results show both staggered line drive and line drive patterns create an immediate peak above 100 STB/D in the production rate which represents approximately 26% of increase in production as a result of pattern reconfiguration.

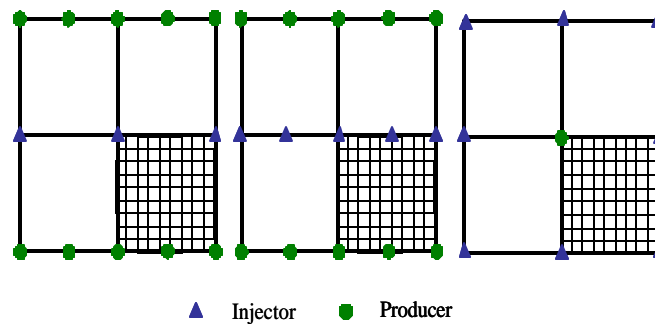


Fig. 18—(a) staggered line drive, (b) line drive and (c) nine-spot well pattern

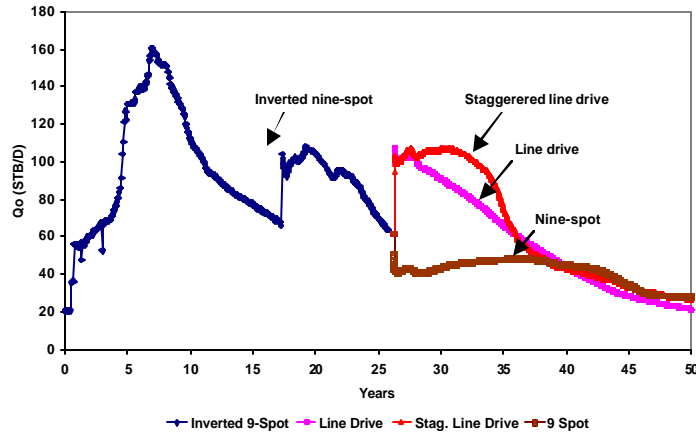


Fig. 19—Comparison of oil rate between staggered line drive, line drive and nine-spot well patterns

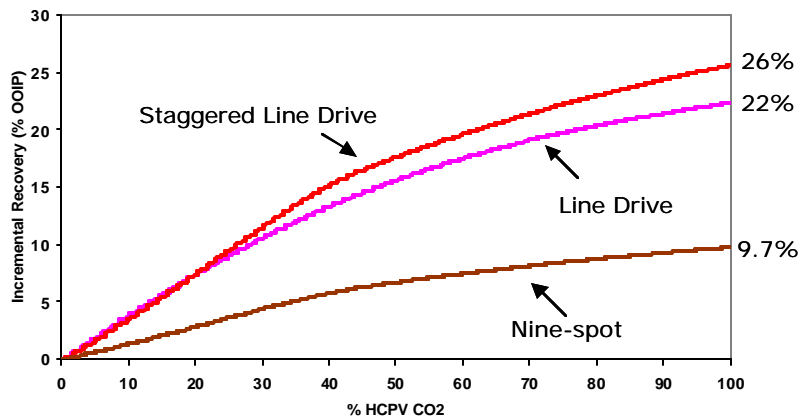


Fig. 20—Comparison of incremental oil recovery between different well pattern configurations

The inverted nine-spot pattern shows the lowest incremental oil recovery among other patterns considered in this study. The low oil recovery clearly indicates that this pattern configuration does not perform well for this particular heterogeneous formation and does not improve the CO₂ displacement.

Conclusions

1. Recovery from a WAG process is a function of the injection rate as well as WAG ratio and the CO₂ slug.
2. WAG injection is effective in increasing the sweep efficiency of the injected CO₂ in the reservoir.
3. The injection of viscous water and polymer resulted in a positive production response that yielded an incremental oil recovery of 32% and 20% respectively.

4. Modeling suggests that pattern conversion from the inverted nine-spot pattern to staggered line drive improves the production oil rate up to 26%.

Acknowledgement

The authors wish to thank the US Department of Energy (Project DE-FC26-01BC15361) for sponsoring this project.

References

1. Chakravarthy, D., Muraidharan, V., Putra, E., and Schechter, D.S. (2004). **Application of X-Ray CT for Investigating CO₂ and WAG Injection in Fractured Reservoirs.** CIPC 2004-232, Annual Technical Meeting,

- Calgary, Canada, 8-10 June.
2. Christman, P.G. and Gorell, S.B. (1988). **A Comparison of Laboratory and Field-Observed CO₂ Tertiary Injectivity**. SPE/DOE 17335, Improved Oil Recovery Symposium, Tulsa, OK, 17-20 April.
 3. Fevang, O., Singh, K. and Whitson, C.H. (2000). **Guidelines for Choosing Compositional and Black-Oil Models for Volatile Oil and Gas Condensate Reservoirs**. SPE 63087, Annual Technical Conference and Exhibition, Dallas, TX, 1-4 October.
 4. Fleming, E.A., Brown, L.M. and Cook, R.L. (1992). **Overview of Production Engineering Aspects of Operating the Denver Unit CO₂ flood**. SPE/DOE 24157, Improved Methods for Oil Recovery, Tulsa, OK, 22-24 April
 5. Ghauri, W.K. (1979). **Production Technology Experience in a Large Carbonate Waterflood, Denver Unit, Wasson San Andres Field**. SPE 8406, Annual Technical Conference and Exhibition, Las Vegas, Sept. 23-26.
 6. Green, D.W. and Willhite, P. (1998). **Enhanced Oil Recovery**. *SPE Textbook Series*, 6.
 7. Harpole, K.J. and Hallenbeck, L.D. (1996). **East Vacuum Grayburg San Andres Unit CO₂ Flood Ten Year Performance Review: Evolution of a Reservoir Management Strategy and Results of WAG Optimization**. SPE 36710, Annual Technical Conference and Exhibition, Denver, Colorado, 6-9 October.
 8. Holm, W. L. (Nov. 1987). **Evolution of the Carbon Dioxide Flooding Processes**. *OGI*
 9. Hsu, C.F., Morell, J.I., and Falls, A.H. (1995). **Field Scale CO₂ Flood Simulations and Their Impact on the Performance of the Wasson Denver Unit**. SPE 29116, Symposium on Reservoir Simulation, San Antonio, TX, 12-15 February.
 10. Huang, E.T.S. and Holm, L.W. (Feb 1988). **Effect of WAG Injection and Rock Wettability on Oil Recovery during CO₂ Flooding**. *SPE*, pp. 119-129.
 11. Jackson, D.D., Andrews, G.L., and Claridge, E.L. (1985). **Optimum WAG Ratio vs. Rock Wettability in CO₂ Flooding**. SPE 14303, Las Vegas, 22-25 Sept.
 12. Jarrel, P.M., Fox, C.E., Stein, M.H. and Webb, S.L.: F. (2002): **Practical Aspects of CO₂ Flooding**, *Monograph Series*, 22.
 13. Khan, S.A., Pope, G.A., and Sepehrnoori, K. (1992). **Fluid Characterization of Three-Phase CO₂/Oil Mixtures**. SPE/DOE 24130, Symposium Oil Recovery, Tulsa, OK, 22-24 April.
 14. Kulkarni, M. M and Rao, D. N. (2004). **Experimental Investigation of Various Methods of Tertiary Gas Injection**. SPE 90589, Annual Technical Conference and Exhibition, Houston, TX, Sept 26 – 29.
 15. Martin, F.D. and Taber, J.J. (April 1992). **Carbon Dioxide Flooding**. *SPE Technology Today Series*, pp. 396 – 400.
 16. Mathis, R.L. (1986). **Reservoir Geology of the Denver Unit-Wasson San Andres Field, Gaines and Yoakum Counties, Texas**. *Permian Basin SEPM Publication* 86-26, 43-47.
 17. Mathis, R.L. and Sears, S.O. (1984). **Effect of CO₂ Flooding on Dolomite Reservoir Rock, Denver Unit, Wasson (San Andres) Field, TX**. SPE 13132, Annual Technical Conference and Exhibition, Houston, TX, September 16-19.
 18. Merrill, R.C., Hartman, K.J., and Creek, J.L. (1994). **A Comparison of Equation of State Tuning Methods**. SPE 28589, Annual Technical and Exhibition, New Orleans, LA, 25-28 September.
 19. Peng, D.Y. and Robinson, D.B. (1976). **A New Two-Constant Equation of State**. *Ind. & Eng. Chem. Fund.* 15, 1, 59-64.
 20. Rogers, J.D. and Grigg, R.B. (2000). **A Literature Analysis of the WAG Injectivity Abnormalities in the CO₂ Process**. SPE 73830, Improved Oil Recovery Symposium, Tulsa, 3-5 April.
 21. Sanchez, N.L. (1999). **Management of Water Alternating (WAG) Injection Projects**. SPE 53714, Latin American and Caribbean Petroleum Engineering Conference, Caracas, Venezuela, 21-23 April.
 22. Swift, T.E., Goodrich, J., Kumar, R., and McCoy, R.L. (1981). **San Andres Reservoir Pressure Coring Project for Enhanced Oil Recovery Evaluation, Bennett Ranch Unit, Wasson Field, West Texas**. SPE/DOE 9798, Symposium on Enhanced Oil Recovery, Tulsa, OK, 5-8 April.
 23. Tanner, C.S. and Baxley, P.T. (1992). **Production Performance of the Wasson Denver Unit CO₂ Flood**. SPE 24156, Enhanced Oil Recovery Symposium, Tulsa, OK, 22-24 April.
 24. Thai, B.N., Hsu, C.F., Bergersen, B.M., Albrecht, S. L., and Richardson, T.W. (2000). **Denver Unit Infill and Pattern Reconfiguration Program**. SPE 59548, Permian Basin Oil and Gas Recovery Conference, Midland, TX, 21-23 March.
 25. Whitson, C.H. (1983). **Characterizing Hydrocarbon Plus Fraction**. *SPEJ*, 23, 683-84.